ELSEVIER

Journal of Alloys and Compounds 330–332 (2002) 787–791

Journal of ALLOYS AND COMPOUNDS

www.elsevier.com/locate/jallcom

Influence of stoichiometry and composition on the structural and electrochemical properties of AB_{5+y}-based alloys used as negative electrode materials in Ni–MH batteries

M. Latroche[a,*], Y. Chabre[b], A. Percheron-Guégan[a], O. Isnard[c], B. Knosp[d]

[a]*UPR 209, LCMTR, ISCSA, IFR 1780, CNRS, 2–8, rue Henri Dunant, 94320, Thiais, France*
[b]*LSP, Université J. Fourier Grenoble I et CNRS, BP 87, 38402, St Martin d'Hères, France*
[c]*CRG-A, D1B, Institut Laue-Langevin, BP 156X, 38042, Grenoble, France*
[d]*SAFT, Direction de la Recherche, 111 Bd. Alfred Daney, 33074, Bordeaux, France*

Abstract

Negative electrodes of Ni–MH batteries are made of AB_5-type based pseudo-binary phases such as $MmNi_{3.55}Mn_{0.4}Al_{0.3}Co_{0.75}$ (Mm=mischmetal). Recently, the appearance of an intermediate γ phase during the charge process for Co-rich alloys was reported. The occurrence of this phase leads to a significant reduction of the decrepitation induced by large volume expansion during charge–discharge cycles and subsequent sensitivity to corrosion. It was also reported that stoichiometries larger than five improve the cycle life of materials with low Co content. In the present work, the structural and electrochemical behaviour of over-stoichiometric low Co content electrode material has been investigated by in situ neutron diffraction. This technique allows bulk analysis of the working electrode and gives information on the involved phases, their relative amount and their structural properties. From this analysis, it has been possible to relate the appearance of the intermediate γ phase to the composition and the stoichiometry of the intermetallic compound. Subsequently, a tentative phase diagram has been established as a function of cobalt content, amount of cerium and stoichiometry ratio *B*/*A*.

Keywords: Intermetallic alloys; Hydrides; Electrode material; Neutron diffraction

1. Introduction

Ni–MH batteries have now widely replaced Ni–Cd batteries in the huge market of portable goods. Most of the negative electrodes of such batteries are made of $LaNi_5$-type alloys [1,2] and improved materials have been obtained from complex pseudo-binary phases such as $MmNi_{3.55}Mn_{0.4}Al_{0.3}Co_{0.75}$ [3,4]. Use of mischmetal was formerly only for economic purpose since this rare earth mixture is cheaper than pure lanthanum, but it appears that the mischmetal composition is also of great importance for cycle lifetime [5]. Even when using mischmetal, alloy cost is still high, especially because of cobalt addition which represents 10% of the weight but 45% of the total alloy price. However, interest in cobalt addition has been demonstrated in the past [6] and recent studies have shown that it plays an essential role in the improvement of cycle life without significant capacity loss for hundreds of cycles [7,8]. In a previous paper [9], we have presented results obtained on different Co-containing electrodes. The appearance of an intermediate γ phase during the charge process for the Co-rich alloys was observed. This phase presents the same structure as the parent intermetallic compound (hexagonal $CaCu_5$ type structure with *P6*/*mmm* space group) but with an intermediate cell volume between the α and β phases which allows one to estimate its hydrogen content at ~3 H/f.u. It was proposed that the occurrence of this intermediate phase, which involves a two step process in the α to β transformation, leads to a significant reduction in the decrepitation induced by the large volume expansion during charge–discharge cycles and the subsequent sensitivity to corrosion. Recently, Cocciantelli et al. [10,11] reported on the influence of the stoichiometric ratio *B*/*A* on the performance of negative electrodes. They came to the conclusion that the use of over-stoichiometric alloys is a promising way to reduce corrosion and that it should compensate for a Co content reduction. Consequently, the question arises if the en-

*Corresponding author. Fax: +33-1-4978-1203.
E-mail address: michel.latroche@glvt-cnrs.fr (M. Latroche).

0925-8388/02/$ – see front matter
PII: S0925-8388(01)01490-6

Table 1
Characterisation of the alloy by EPMA and XRD analysis

Electron probe micro analysis (±0.01)	B/A ratio	Cell parameters		Volume, V (Å^3)
		a (Å)	c (Å)	
$La_{0.51}Ce_{0.22}Nd_{0.22}Pr_{0.017}Ni_{3.99}Mn_{0.38}Al_{0.29}Co_{0.36}$	5.19	5.001(1)	4.054(1)	87.783(5)

Numbers between parentheses correspond to the estimated standard deviations (esd's).

hanced behaviour of these electrodes is related to the benefit effect of the γ phase.

In the present paper, we will present results on the influence of the stoichiometry and the composition on the appearance of the γ phase. A tentative phase diagram will be proposed taking into account amount of cobalt, Ce/La ratio and stoichiometry ratio B/A.

2. Experimental details

The alloy was prepared by induction melting of the pure components (rare earths, nickel, cobalt: 3 N; manganese, aluminium: 4 N) under vacuum in a water cooled copper crucible. The alloy was turned over five times to ensure good homogeneity and was annealed for 4 days at 1050°C. Sample was characterised by metallographic examination and microprobe analysis (EPMA). X-ray diffraction (XRD) pattern was obtained on a Bruker D8 Advance diffractometer using Cu Kα radiation and was indexed in the $CaCu_5$ hexagonal cell (*P6/mmm* space group). Results of the characterisation for the over-stoichiometric sample are given in Table 1.

Pressure–composition–isotherm (P–C–I) curve was measured with D_2 gas as deuterium is used for neutron diffraction. About 0.5 g of sample was ground mechanically under argon and activated by five solid-gas cycles. The absorption–desorption isotherm curve was determined by Sieverts' method.

Neutron diffraction experiments were performed at room temperature on the D1B instrument at the Institut Laue Langevin in Grenoble. Wavelength was set to 2.523 Å and the patterns were recorded every 20 min with a position sensitive detector in the range $28° < 2\theta < 108°$ in steps of 0.2°. Diffraction patterns were analysed using the program FULLPROF [12].

The electrode was prepared as described in Ref. [9]. However, for the present in-situ study, with the aim of improving the design, counter electrodes were located on both sides of the working electrode plate, as in cylindrical batteries. Thus the working electrode is a 10-mm diameter cylinder made of one roll of active material pasted grid sandwiched between inner (∅ 8 mm) and outer (∅ 12 mm) counter-electrode cylinders made of nickel grid, with silica sheaths as separators on each side of the working electrode. Such an electrode assembly leads to current lines comparable to those of prismatic design. It ensures homogeneous current density keeping the cylindrical geometry necessary for neutron diffraction, with a sufficiently large amount of active material (2–3 g). The electrode was immersed in NaOD 5.5 N electrolyte and the reference electrode ($Cd/Cd(OH)_2$) was in a side tube entering the main tube with a capillary going against the bottom side of the working electrode. The cell was controlled with a VMP multichannel potentiostat-galvanostat (Bio-Logic).

Before starting the in situ experiments, the electrode was galvanostatically activated by two cycles at C/10-D/10 plus three cycles at C/5-D/5 followed by a final potentiostatic discharge at 0.3 V versus the reference electrode to obtain the nominal electrochemical capacity (see caption of Table 2 for the meaning of C/n or D/n). This capacity was found in good agreement with that expected from P–C–I curve. The results from solid-gas measurement and activation protocol are detailed in Table 2. The in situ electrochemical protocol consisted of a C/15 charge for 25 h

Table 2
Parameters for the studied electrode

P_{des}, bar	C (S.G.) $P_{eq}=1$ bar, D/mol (mAh/g)	Active mass, g	Capacity after Dp(0.3), mAh/g	Activation ex situ
0.24	4.21 (270)	2.474	258	Two cycles C/10-R-D/10 + three cycles C/5-R-D/5 + Dp(+0.3)

The solid-gas (SG) capacity is measured under 1 bar of deuterium gas (i.e. in the β phase domain) and converted into electrochemical units (mAh/g). The discharge electrochemical capacity is measured from the last discharge Dp(+0.3). C/n (D/n) stands for nominal capacity galvanostatically charged (discharged) in n hours. Dp(E) means a potentiostatic discharge at constant potential e (in V) versus a $Cd/Cd(OH)_2$ reference electrode and R corresponds to an open circuit relaxation.

followed by a relaxation time of 1.5 h. The discharge was then started at the same rate (D/15) with a cut-off potential of +0.3 V versus the reference electrode.

Cycle life experiments have been measured using negative limited vented cells with sintered $Ni(OH)_2$ positive electrodes, polyamide separator and negative pellet electrode. The cycle tests were performed at 1 C rate with 80% of depth of discharge.

3. Results

The three-dimensional view in Fig. 1 shows the evolution of the diffraction patterns during the in situ C/15 charge. The progressive disappearance of the α phase peaks and the appearance of the peaks of the β phase are observed. Moreover, on the right part of the figure, at $2\theta = 75.5°$, the appearance and disappearance of one peak belonging to the γ phase is clearly seen. It is worth noting that the γ and β peaks have a nearly constant 2θ position (i.e. a nearly constant cell volume), whereas the α phase peaks move from the beginning of the charge.

The electrode behaviour is presented in Fig. 2 for a complete cycle of charge and discharge (C/15-D/15). In the upper part (Fig. 2a), the relative amounts of each phase are shown together with the total quantity of Coulomb (right scale) having crossed the cell (Q in mAh/g). It is important to note that upon charge Q represents the sum of the intrinsic capacity of the alloy and the quantity of recombined deuterium at the surface of the negative electrode.

For the first hours of charge, the classical behaviour for a two-phase system is observed. The α phase amount rapidly decreases whereas the hydride γ phase appears. However, after 5 h, new diffraction peaks are observed and it is necessary to add a third phase (β) to correctly refine the patterns. The amount of the γ phase reaches a maximum of 45% after 12 h before it decreases to attain ~20% at the end of the charge. In the mean time, the β phase proportion reaches 70% whereas the α phase correspondingly disappears. Between $5 < t < 20$ h, the cell volumes for the β and γ phases remain nearly constant (Fig. 2b), which is characteristic of phase equilibrium behaviour.

After a short relaxation time, a galvanostatic discharge at a rate of D/15 was performed. In contrast to the charge, a fast decrease of the β phase volume from 104 to 97 $Å^3$ is seen for the beginning of the discharge (Fig. 2). This behaviour is typical for solid solution and corresponds to the decrease of the β phase deuterium concentration. Consequently, the diffraction peaks of the phases γ and β rapidly merge and cannot be distinguished anymore. Therefore, the data refinement was performed assuming only two phases: β(γ) and α (Fig. 2).

4. Discussion

From our present study, it is found that the γ phase is observed in over-stoichiometric 5wt.%Co alloy whereas it was not the case in stoichiometric 5wt.%Co alloy studied in Ref. [9]. Moreover, the γ phase was also observed in the stoichiometric compound with 10wt.%Co [9]. It is therefore concluded that the probability of appearance of the γ phase decreases with cobalt content but increases with over-stoichiometry. Following this idea, the data collected on various $Mm(Ni,Mn,Al,Co)_{5+y}$ material electrodes are compared in Table 3. From this data, a tentative three-dimensional diagram showing the different compositions where the γ phase was (or was not) observed as a function of Co amount, Ce/La ratio and stoichiometry ratio B/A, is given in Fig. 3. It appears that a certain amount of cerium

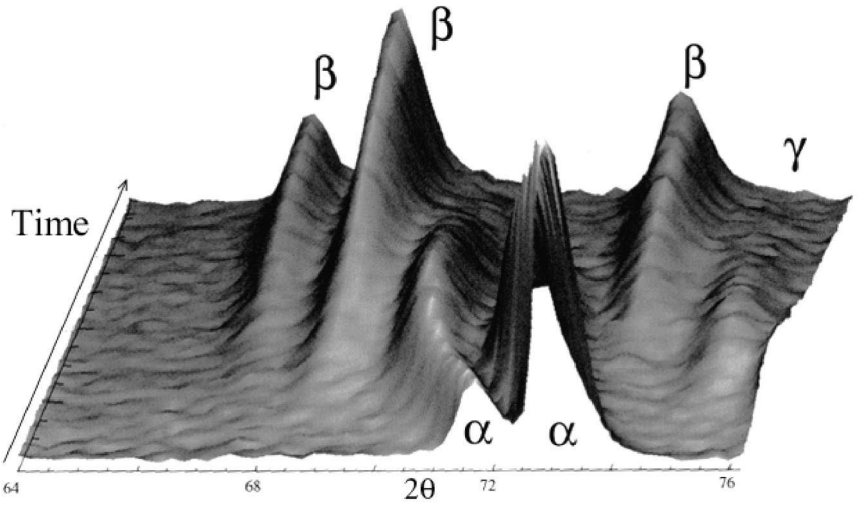

Fig. 1. Three-dimensional view of the diffraction patterns of the working electrode during the C/15 charge between 64 and 76° (2θ). One can note the appearance and disappearance of a peak belonging to the γ phase at $2\theta = 75.5°$ on the right of the plot.

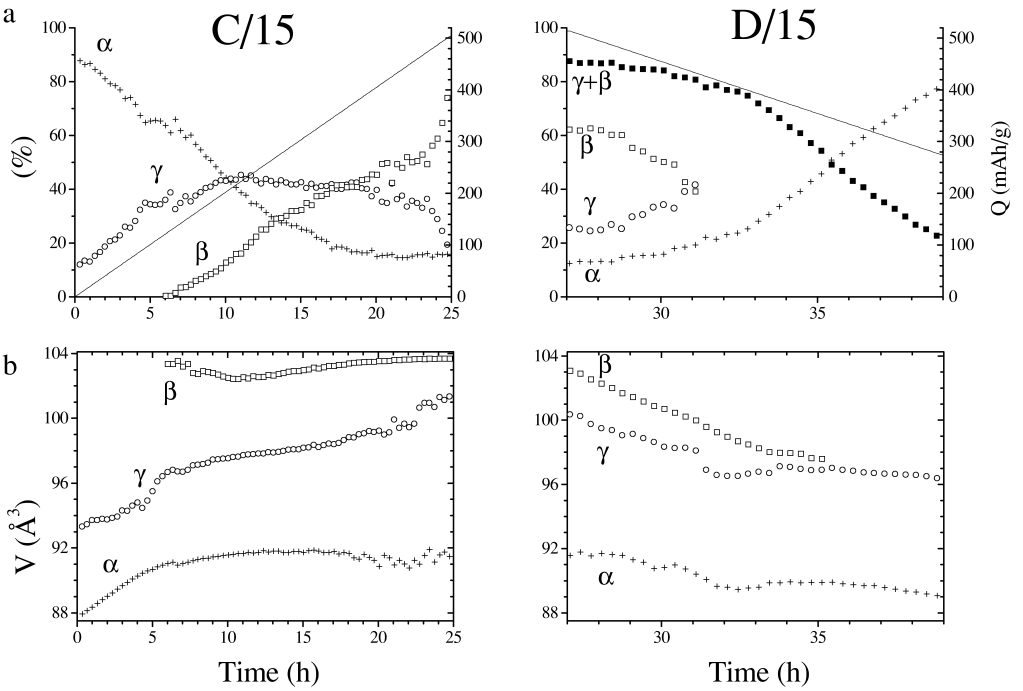

Fig. 2. Electrochemical charge/discharge cycle of the electrode. (a) Amount of phases α (+), γ (○) and β (□) and capacity *Q* (—) (right scale). (b) Cell volume for phases α (+), γ (○) and β (□). The charge capacity reaches 500 mAh/g but including the D_2 gas evolving during charge. The discharge capacity is estimated to 500−260=240 mAh/g in agreement with the data reported in Table 2.

Table 3
Summary of the different compositions studied by in situ neutron diffraction

Ref.	*V*	*M*	%wt.Co	Ce/La	*B*/*A*	γ
[13]	89.90	425.72	10.5	0.00	5.06_0	
[9]	88.11	423.88	5.0	0.44	5.05_9	
[9]	88.24	422.94	9.9	0.46	5.04_1	*
[9]	88.32	423.70	10.5	0.44	5.04_6	*
This work	87.81	419.97	5.1	0.43	5.19_1	*

The compounds for which the γ phase was observed are indicated by a star (*).

is necessary to allow the γ phase to exist. Cobalt concentration and over-stoichiometry appear inversely correlated. From the cross-section corresponding to a Ce/La ratio=0.45, if one assumes a linear dependence of the two parameters %wt.Co and *B*/*A* ratio, a cobalt-free alloy exhibiting the γ phase could be obtained with the stoichiometry $AB_{5.34}$.

Interest in the γ phase has been described in Ref. [9]. This intermediate deuteride involves a two step process in the α to β transformation. It reduces the decrepitation process induced by the large volume expansion observed

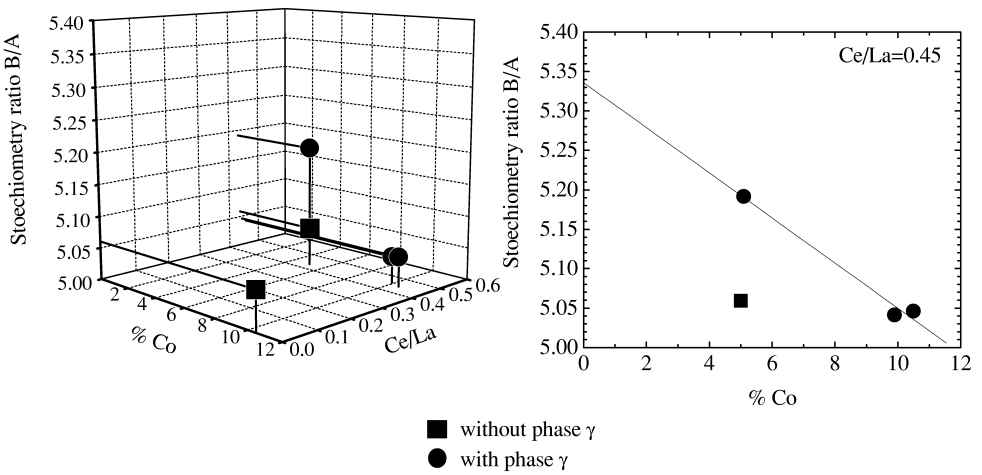

Fig. 3. Three-dimensional diagram showing the different compositions where the γ phase was observed as a function of Co rate, Ce/La ratio and stoichiometry ratio *B*/*A*. The right part of the figure. shows the line extrapolated to zero Co content for a Ce/La ratio close to 0.45.

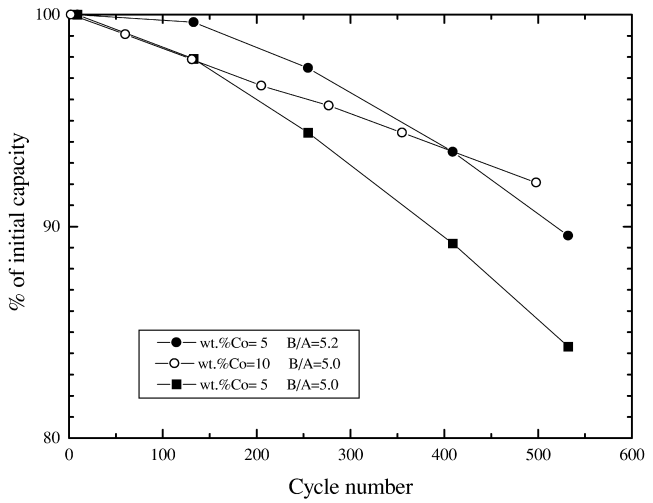

Fig. 4. Cycle life behaviour of different electrodes (Ce/La ratio = 0.45) as a function of cobalt concentration and stoichiometry ratio *B*/*A*. The samples for which the γ phase is present are represented by circles.

during charge–discharge cycles and responsible for corrosion. To support this hypothesis, the cycle life of three compounds with various composition have been tested. The results are shown in Fig. 4. The two compounds for which the γ phase have been reported exhibit better cycle life behaviour.

5. Conclusions

To conclude, alloys with appropriate compositions as regards the Ce/La ratio, over-stoichiometry and cobalt content exhibit intermediate γ phase. This phase plays an important role in the reduction of the decrepitation process and consequently, on corrosion and cycle life. Combination of over-stoichiometry and low Co content can be achieved to design low cost and high-performance electrode material for Ce/La ratio ~ 0.45. It will be valuable in the future to determine the lower limit for the Ce/La ratio in order to fully establish the domain of existence of the γ phase.

References

[1] A. Percheron-Guégan, J.C. Achard, J. Sarradin, G. Bronoël, Electrode material based on lanthanum and nickel, electrochemical uses of such materials, French patents 75 16160 (1975), and 77 23812 (1977); US patent 688537 (1978).
[2] J. Bouet, B. Knosp, A. Percheron-Guégan, J.M. Cociantelli, Matériau Hydrurable pour Electrode Négative d'Accumulateur Nickel-Hydrure, French patent 92 14662 (1992).
[3] H. Ogawa, M. Ikoma, H. Kawano, I. Matsumoto, Power Sources 12 (1988) 3931.
[4] M. Ikoma, H. Kawano, I. Matsumoto, N. Yanagihara, Eur. Patent Appl. No 0 271 043 (1987).
[5] G.D. Adzic, J.R. Johnson, J.J. Reilly, J. McBreen, S. Mukerjee, J. Electrochem. Soc. 142 (1995) 3429.
[6] J.J.G. Willems, Philips J. Res. 39 (Suppl. 1) (1984) 1–94.
[7] J.M. Cocciantelli, P. Bernard, S. Fernandez, J. Atkin, J. Alloys Comp. 253–254 (1997) 642–647.
[8] G.D. Adzic, J.R. Johnson, S. Mukerjee, J. McBreen, J.J. Reilly, J. Alloys Comp. 253–254 (1997) 579–582.
[9] M. Latroche, A. Percheron-Guégan, Y. Chabre, J. Alloys Comp. 293–295 (1999) 637–642.
[10] J.-M. Cocciantelli, P. Leblanc, G. Caillon, B. Knosp, P. Blanchard, J. Atkin, J. New Mater. Electrochem. Syst. 2 (1999) 151.
[11] J.-M. Cocciantelli, C. Arquey, A. Percheron-Guégan, Brevet No. FR 9709568.
[12] J. Rodríguez-Carvajal, in: Abstracts of Satellite Meeting on Powder Diffraction, Congress of the International Union of Crystallography, Toulouse, France, 1990, p. 127.
[13] M. Latroche, A. Percheron-Guégan, Y. Chabre, J. Bouet, J. Pannetier, E. Ressouche, J. Alloys Comp. 231 (1995) 5375.